Behavior of the nonlinear refractive indices and birefringence in the neighborhood of first- and second-order phase transitions in lyotropic liquid crystals

F. L. S. Cuppo, S. L. Gómez, and A. M. Figueiredo Neto
Instituto de Física, Universidade de São Paulo, Caixa Postal 66318, 05315-970 São Paulo, São Paulo, Brazil
(Received 13 December 2002; published 29 May 2003)

We investigated the behavior of the nonlinear refractive indices (n_2) and birefringence (Δn_2) in the vicinity of the nematic-to-isotropic (N-I) and nematic uniaxial-to-nematic biaxial (N-N) phase transitions in a lyotropic liquid crystal. The single-beam Z-scan technique is used to measure n_2 in different relative configurations of the electric field of the laser beam and the symmetry axes of the phases. In the N-I transition, the nonlinear optical birefringence shows a discontinuity at the transition temperature (T_c), as observed in the linear birefringence. On the other hand, in the N-N transition, Δn_2 was shown to be proportional to $|T-T_c|^{-\beta}$, with $\beta \sim 0.5$, in both uniaxial and biaxial nematic domains. No discontinuity was observed on Δn_2 in the N-N transition. The symmetric invariants of the order parameter were shown to be linear functions of the temperature in the uniaxial nematic domain, in good agreement with the mean-field prediction.

DOI: 10.1103/PhysRevE.67.051711 PACS number(s): 61.30.St, 42.65.−k, 78.20.Ci

I. INTRODUCTION

In a seminal work, Yu and Saupe [1] have put in evidence the existence of a biaxial nematic phase (N_B) in between two uniaxial nematic phases [N_D (discotic) and N_C (calamitic)] in a lyotropic liquid crystalline system composed of two types of amphiphilic molecules and water. In the neighborhood of these nematic phases, isotropic phases (I) are often present. This topology of phase diagram was found in other ternary lyotropic mixtures [2,3], being a characteristics of lyotropics and never encountered in thermotropic liquid crystals. An interesting subject of research in the field of phase transitions and statistical mechanics is the nature of the nematic-to-nematic and nematic-to-I transitions. Usually, these transitions are studied measuring the invariants ($\sigma_i, i=1,2,3$) of the anisotropic part of the optical dielectric tensor $\vec{\vec{\epsilon}}_a$, chosen as the symmetry-breaking order parameter [4], commonly written in terms of the linear optical birefringences Δn_L and δn_L. Galerne and Marcerou [5] measured both Δn_L and δn_L in the KL-DeOH-W (KL is potassium laurate, DeOH is decanol, and W stands for water), lyotropic mixture, in the temperature range $\Delta T/T_c \sim 3\times 10^{-3}$ from the temperature transitions T_c] and calculated the invariants of $\vec{\vec{\epsilon}}_a$. One of these invariants (σ_1) is trivially zero since, in this framework, the anisotropic part of the dielectric tensor is traceless. The two other invariants are functions of the temperature and presented a linear behavior in the uniaxial and biaxial nematic phase domains, in the vicinity of the phase transitions. Their results show that the uniaxial-to-biaxial transition is second order and mean-field and the nematic-to-I transitions are weakly first order, with the linear optical birefringence presenting a discontinuity in T_c. Saupe and co-workers [6,7] measured, in the same lyotropic mixture, one of the birefringences at the N_B and N_C phases and observed small deviations from the mean-field behavior at the uniaxial-to-biaxial phase transition, in a temperature range of $\Delta T/T_c \sim 10^{-4}$ from T_c. The critical exponents of the order parameter (β) and of the susceptibility (γ) of the KL-DeOh-W mixture were found to be $\beta=0.38(3)$ and $\gamma=1.29(6)$ (the theoretical predictions of the XY model are [8] $\beta=0.38$ and $\gamma=1.35$). The uniaxial-to-biaxial phase transition in lyotropics was also investigated by Lacerda Santos and co-workers [9] using the Rayleigh scattering technique, observing thermally excited biaxiality fluctuations appearing in the uniaxial N_D phase. A critical slowing down of these biaxiality fluctuations was evidenced.

Contrarily to the linear optical properties of lyotropics that have been extensively investigated, the nonlinear optical behavior of these systems is not completely understood. An elegant method to measure the nonlinear response of a medium is the *Z-scan* technique [10], where the sample is moved through the focal region of a single focused Gaussian laser beam, along the direction of the beam propagation (z axis). The transmitted light intensity in the far field is measured as a function of sample position. It is used to measure the nonlinear refractive index (n_2) of a sample assuming that the refractive index can be written as $n=n_L+n_2 I$, where n_L is the linear index of refraction and I is the incident light intensity on the sample. Depending on the time scale of the experiment, different mechanisms can be studied: the optical Kerr effect, the third-order (and higher-orders) nonlinear electronic polarization, thermal effects, etc. In a previous work [11] we studied the nonlinear response, in time scales of milliseconds, of a sample of the KL-DeOH-W mixture in the N_C phase (fixed temperature) and measured $n_2 \sim -10^{-6}$ esu, which is 10^2 smaller than that measured in thermotropics [12]. In both conditions of the laser electric field, parallel and perpendicular to the nematic director, $n_2<0$, indicating the defocusing behavior of the sample. Considering the particularities of the lyotropic system and the time scale used, we suggested that the nonlinear response observed is mainly from thermal origin. To the best of our knowledge, however, no investigations of these properties were reported in the vicinity of the nematic-to-nematic (N-N) lyotropic phase transitions. In this work we study the behavior of the nonlinear refractive indices and birefringence of the KL-DeOH-W lyotropic mixture in the neighborhood of first- (nematic-to-I) and second- (N-N) order phase tran-

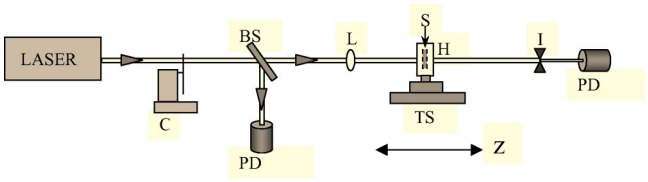

FIG. 1. Sketch of the *Z*-scan apparatus: *C*, chopper; BS, beam splitter; *L*, lens; PD, photo detector; TS, translation stage; *S*, sample; *H*, temperature controlled device; *I*, iris.

sitions, by using the *Z*-scan technique. The experimental data are discussed in the framework of the Landau–de Gennes mean-field theory.

II. EXPERIMENTAL SECTION

A. The *Z*-scan technique

The *Z*-scan apparatus is the usual one described elsewhere [10–12]. Although many techniques have been developed to study nonlinear optical effects, the single-beam *Z*-scan technique stands up because of its simplicity and sensitivity in measuring both the sign and the magnitude of the nonlinear refraction index. In this technique a polarized Gaussian laser beam, propagating in the *z* direction, is focused to a narrow waist by using a lens. The sampled is moved along the *z* direction through the focal point and the transmitted intensity is measured in the far field on the axis of the propagating direction, as function of the *z* position. As the sample moves along the beam focus, self-focusing or defocusing modifies the wave front phase, thereby modifying the detected intensity. The great advantage of the *Z*-scan technique is that it allows a straightforward determination of the magnitude and sign of the nonlinear phase shift $\Delta\Phi_o$ introduced by the sample from the peak-to-valley difference (ΔT_{pv}) in the *Z*-scan curve. For a sample where nonlinear absorption is negligible, the on-axis normalized transmittance T_N, as a function of the sample position $x=z/z_o$ (where z_o is the Rayleigh range of the Gaussian beam), is given approximately by [10]

$$T_N(z)\simeq 1+\Delta\Phi_o\frac{4x}{(1+x^2)(9+x^2)}, \qquad (1)$$

with $\Delta\Phi_o=(2\pi d/\lambda)(n_2/\varepsilon_o c n_L)I_o$ and $\Delta T_{pv}=0.406|\Delta\Phi_o|$, where ε_o and c are the permittivity of free space and the speed of light, respectively, d is the sample thickness, and I_o is the light intensity at the focus.

In our *Z*-scan setup [11], sketched in Fig. 1, a solid state cw Millennia laser ($\lambda=532$ nm) is used. A mechanical chopper is placed in the beam path, before the sample, to modulate its intensity, providing nearly square pulses with a pulse width of 25 ms (i.e., 25 ms in the ''on'' state, with the laser shining the sample, and 25 ms in the ''off'' state). The power of the beam ranges from 100 to 250 mW; typical beam waist at the sample is 25 μm. A signal acquisition, with temporal resolution, is made to discard the linear effects [13].

B. The samples

The samples investigated are from the mixture of KL-DeOH-*W*, at the corresponding concentrations in weight percentage: a sample named SI [30.85/6.88/62.27] and a sample named SN [30.77/6.55/62.68]. The phase sequences of both samples SI and SN are ($\lesssim 15\,^\circ$C)$N_C(T_{cI}=42.6\,^\circ$C)I and ($\lesssim 17\,^\circ$C) $N_C(T_{c1}=25.02\,^\circ$C)$N_B(T_{c2}=46.31\,^\circ$C)N_D ($\gtrsim 52\,^\circ$C), respectively. The width of the N_C-to-I transition in sample SI is $\sim 1\,^\circ$C. Samples are encapsulated in rectangular glass cells of sample thickness $d=200$ μm, placed in a temperature controlled device (accuracy of $\pm 0.1\,^\circ$C). The local heating of the sample due to the laser beam at the focus position is evaluated to be $\sim 0.2\,^\circ$C. In these conditions, we fixed the step between successive temperatures in our experiment in $\Delta T=0.2\,^\circ$C. Samples at the N_C phase are oriented initially in an electromagnet (static field of 10 kG for some hours) at $T\sim 20\,^\circ$C, outside the *Z*-scan setup, taking advantage also of the surface orienting effect. This sample orients with the nematic director parallel to the magnetic field ($\vec{B}$). In the case of the N_B phase, the long axis of the anisotropic micelles (which corresponds to the direction of the director in the N_C phase) orients parallel to the magnetic field and the two optical axes of the phase are in the plane perpendicular to the biggest surface of the sample holder, which contains $\vec{B}$ [14]. The orientation of the N_B phase is achieved by the combination of the static magnetic field and the surface orienting effect of the sample-holder walls. After that, it is moved to the *Z*-scan setup where a magnetic field of ~ 1 kG (which defines the *y* axis of the laboratory frame axes) keeps the sample alignment during the experiment. Two different geometries of the laser electric field $\vec{E}$ with respect to $\vec{B}$ are available: parallel ($\parallel$) and perpendicular ($\perp$).

III. RESULTS AND DISCUSSION

Figures 2 and 3 present the measurements of n_2 and the corresponding nonlinear birefringences ($\Delta n_2=n_{2\parallel}-n_{2\perp}=n_2^{(y)}-n_2^{(x)}$), as a function of the temperature, in both configurations of $\vec{E}$ with respect to $\vec{B}$ ($\parallel$ and $\perp$) of sample SI and SN, in the vicinity of the phase transitions. These values are obtained by fitting Eq. (1) to the experimental *Z*-scan curves. Figure 4 presents the measurements of the corresponding linear birefringence ($\Delta n_L=n_{L\parallel}-n_{L\perp}$), as a function of the temperature, of both SI and SN phases.

A. The N_C-to-I phase transition

Let us analyze firstly the N_C-to-I phase transition. The values of n_2 in both configurations are *negative* [Fig. 2(a)]. As previously discussed [15], $n_2\propto\partial n/\partial T$, which is the thermo-optic coefficient. Our results indicate that the sign of the thermo-optic coefficient *remains the same up to* 0.1 °C from T_{cI}. In the N_C phase, $n_{2\parallel}$ shows a stronger dependence on T than $n_{2\perp}$, whose values present a spread of about 0.1×10^{-6} esu around -2.6×10^{-6} esu. The origin of this effect could be the modification of the shape anisotropy of the micelles, principally in the direction of their long axis (or,

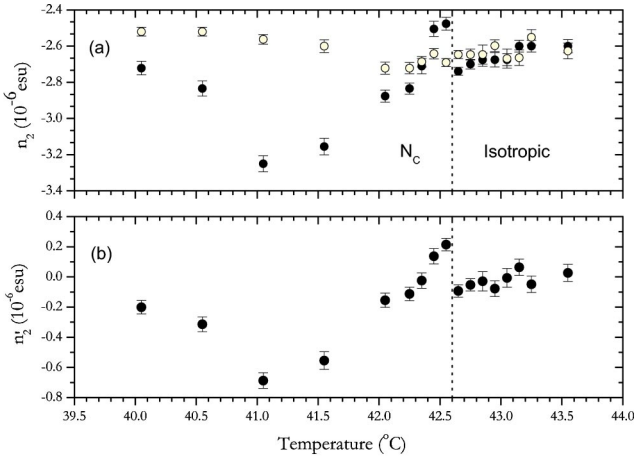

FIG. 2. (a) Nonlinear refractive index n_2 as a function of the temperature in both configurations of $\vec{E}$ with respect to $\vec{B}$, sample SI: (●) $\vec{E}\|\vec{B}$; (○) $\vec{E}\perp\vec{B}$. Dashed line corresponds to $T_{cI}=42.6\,^{\circ}\mathrm{C}$. (b) Nonlinear birefringence ($\Delta n_2=n_{2\|}-n_{2\perp}$) corresponding to the data of Fig. 2(a). Dashed line corresponds to $T_{cI}=42.6\,^{\circ}\mathrm{C}$.

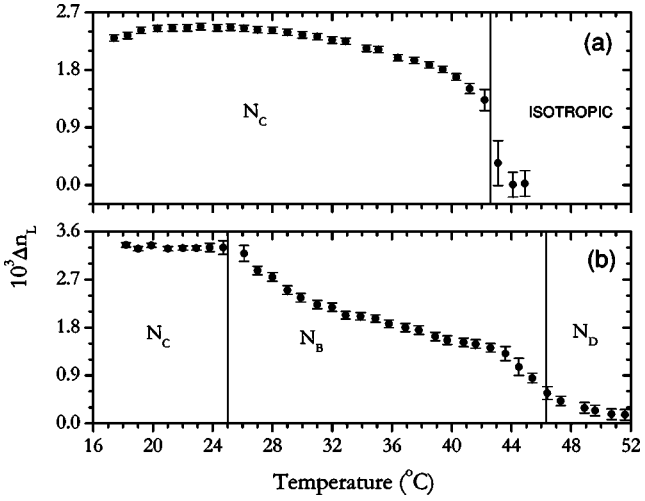

FIG. 4. (a) Linear birefringence ($\Delta n_L=n_{L\|}-n_{L\perp}$) as a function of the temperature of sample SI. Solid line corresponds to $T_{cI}=42.6\,^{\circ}\mathrm{C}$. (b) Linear birefringence ($\Delta n_L=n_{L\|}-n_{L\perp}$) as a function of the temperature of sample SN. Solid lines correspond to $T_{c1}=25.02\,^{\circ}\mathrm{C}$ and $T_{c2}=46.31\,^{\circ}\mathrm{C}$.

the director), as a function of the temperature. In the direction perpendicular to the director, the amphiphilic double layer is not expected to considerably change its dimension in this temperature range, what reflects a weak temperature dependence of $n_{2\perp}$. Our results, however, differ from those reported by Pereira and co-workers using the thermal lens technique in a similar lyotropic sample (thicker than ours) of the same mixture [16], where $(\partial n/\partial T)_{\|}$ changes its sign in a range of about 2 °C from the nematic-to-I transition temperature and $(\partial n/\partial T)_{\perp}$ keeps the same sign. It is important to stress that during our experiment a magnetic field is present to maintain the good orientation of the N_C sample. This is a key point since the sample may disorient during the exposure to the beam. In the N_C phase domain near the transition to the isotropic phase, Δn_2 presents a minimum (negative) value at $T\sim 41\,^{\circ}\mathrm{C}$ and then increases as $T\rightarrow T_{cI}$. It becomes positive, reaches $\Delta n_2^I\sim 0.2\times 10^{-6}$ esu at $(T_{cI}-T)\sim 0.1\,^{\circ}\mathrm{C}$ and vanishes at $T>T_{cI}$. This discontinuity in Δn_2 at $T=T_{cI}$ is compatible with the first-order characteristics of the nematic-to-isotropic phase transition, being also observed in the measurements of the linear birefringence shown in Fig. 4(a).

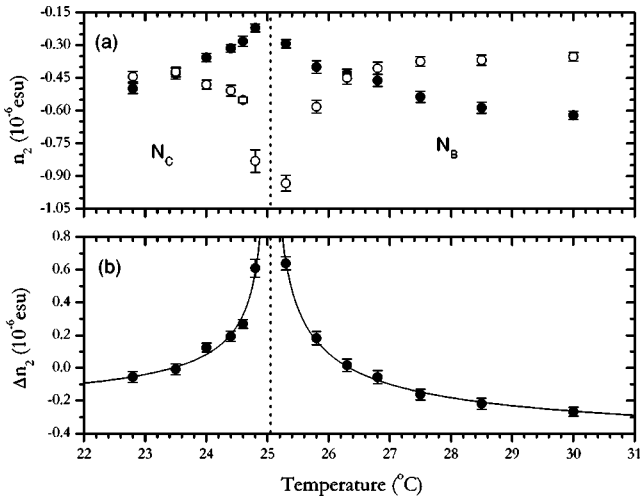

FIG. 3. (a) Nonlinear refractive index n_2 as a function of the temperature in both configurations of $\vec{E}$ with respect to $\vec{B}$, sample SN: (●) $\vec{E}\|\vec{B}$; (○) $\vec{E}\perp\vec{B}$. Dashed line corresponds to $T_{c1}=25.02\,^{\circ}\mathrm{C}$. (b) Nonlinear birefringence ($\Delta n_2=n_{2\|}-n_{2\perp}$) corresponding to the data of Fig. 3(a). Dashed line corresponds to $T_{c1}=25.02\,^{\circ}\mathrm{C}$. The solid and dotted lines correspond to the fitting function $\Delta n_2\propto|T-T_{c1}|^{-\beta}$, with $\beta_C=0.55(3)$ and $\beta_B=0.50(1)$ in the N_C and N_B phases, respectively.

B. The N_C-to-N_B phase transition

Let us face now the nematic-to-nematic transition. Figure 3(a) shows the nonlinear refractive indices n_2 as a function of the temperature, in both configurations of $\vec{E}$ with respect to $\vec{B}$ of sample SN in the vicinity of T_{c1}. Measurements are made in the temperature domains $\Delta T/T_{c1}\sim 7\times 10^{-3}$ and 2×10^{-2}, corresponding to the N_C and N_B phases, respectively. Sample at the N_C phase is oriented with the director parallel to the y axis and at the N_B phase with both optical axes in the yz plane, symmetrically oriented with respect to the z axis. In the studied configurations, $n_2<0$ and present a "singular-type" behavior as $T\rightarrow T_{c1}$ from both sides of the transition temperature: the sign of $\partial n_2/\partial T$ changes at T_{c1}. Let us consider that n_2 is mainly influenced by the variation of the local density (ρ) and the order parameter (S) as a function of the temperature. The singular-type behavior of n_2 in both configurations, as $T\rightarrow T_{c1}$, seems to indicate that fluctuations of ρ and S due to the modifications of the micellar shape anisotropy *and* their orientational fluctuations (which account for the different nematic phases) became more important when the system approaches T_{c1}. The continuous variation of n_2 in both configurations across the tran-

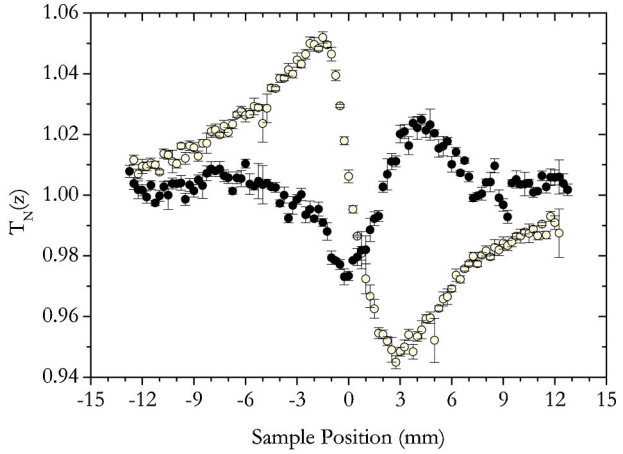

FIG. 5. *Z*-scan normalized transmittance curves of sample SN2, geometry $\vec{E}\|\vec{B}$. (○)$T=31\,^{\circ}\mathrm{C}$, N_C phase; (●)$T=T_{c1}=32\,^{\circ}\mathrm{C}$.

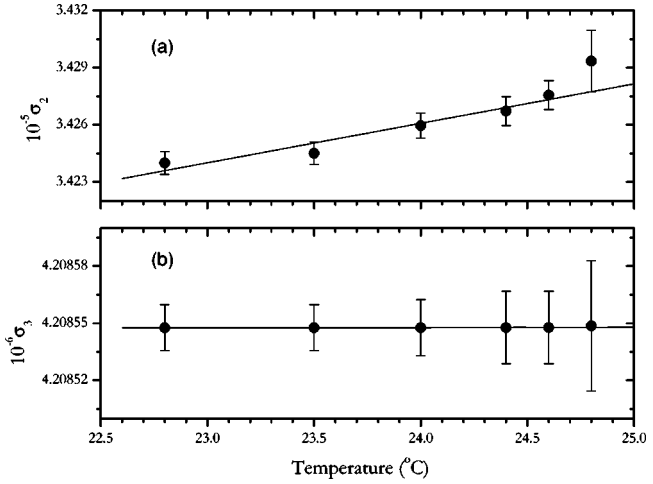

FIG. 6. Symmetric invariants σ_2 (a) and σ_3 (b) as a function of the temperature. Sample SN, N_C phase domain. The solid lines are linear fits.

sition is compatible with the continuous modification of the micellar shape anisotropy previously proposed [14]. This general behavior of n_2 as a function of T was also observed by us at the N_C-to-N_B transition in other lyotropic samples of the same mixture, with different relative concentrations of the compounds. However, concerning the sign of n_2, an interesting result is observed in a sample with the concentrations in weight percent [KL(29.42)-DeOH(6.47)-W(64.11)], named SN2: $n_{2\|}$ continuously decreases its (negative) value, *becomes positive* and then increases its value up to T_{c1} ($=32\,^{\circ}\mathrm{C}$ in this case). Figure 5 shows typical *Z*-scan curves obtained at $T=31\,^{\circ}\mathrm{C}$ (at the N_C phase) and at T_{c1}, in the configuration of $\vec{E}\|\vec{B}$. The inversion of the peak and valley relative positions is a signature of the inversion of the $n_{2\|}$ sign. The origin of this inversion (reported previously in the *N-I* transition [16]) is not completely understood. Figure 3(b) presents the nonlinear birefringence as a function of the temperature in the vicinity of the uniaxial-to-biaxial phase transition of sample SN. In the framework of the mean-field theory, the free energy of the system can be written in terms of σ_i as [5] $F=a\sigma_2+b\sigma_3+\frac{1}{2}d\sigma_2^2+e\sigma_2\sigma_3+\frac{1}{2}f\sigma_3^2$, both invariants being $\propto|T-T_c|$. In the N_C phase,

$$\sigma_2=\frac{8}{27}\bar{n}^2\left[6(\Delta n_L)^2+\left(\frac{E^2}{6}\right)^2(\Delta n_2)^2-E^2\Delta n_L\Delta n_2\right],$$

$$\sigma_3=-\frac{64}{9}\bar{n}^3\left[(\Delta n_L)^3-\left(\frac{E^2}{2}\right)^3(\Delta n_L)^3+\frac{3E^2}{2}(\Delta n_L)^2\Delta n_2+\frac{3E^2}{4}\Delta n_L(\Delta n_2)^2\right],$$

where $\bar{n}$ is the mean index of refraction, $\Delta n=\Delta n_L+(E^2/2)\Delta n_2$ and $\delta n=\delta n_L+(E^2/2)\delta n_2$. In our experimental conditions we measure the birefringences (linear as shown in Fig. 4, measured with the usual conoscopy setup [5] and nonlinear as measured with the *Z*-scan setup) in the *xy* plane. As in this framework, in the biaxial phase domain, $\Delta n_L\propto|T-T_c|^{\pm\beta}$ with $\beta=0.5$, one expects that $\Delta n_2\propto|T-T_c|^{\pm\beta}$. The fitting functions ($\Delta n_2\propto|T-T_c|^{-\beta}$) in Fig. 3(b) have $\beta_B=0.50(1)$ and $\beta_C=0.55(3)$ in the N_B *and* N_C phase domains, respectively. This behavior *in both* uniaxial and biaxial phases is remarkable. From both sides, Δn_2 tends to $\sim 0.9\times10^{-6}$ esu, which is compatible with the characteristics of a second-order phase transition where no discontinuities are expected in the order parameter at T_c. On the other hand, this behavior in the N_C domain is completely different from that of the linear birefringence, which was shown to be almost constant (depending on the particular sample's composition) in the vicinity of the uniaxial-to-biaxial transition [5]. The invariants σ_2 and σ_3 in the N_C domain as a function of the temperature are presented in Figs. 6(a) and 6(b), respectively, in good agreement with the mean-field prediction.

IV. CONCLUSIONS

In summary, we investigated the behavior of the nonlinear refractive indices and birefringence in the vicinity of the nematic-to-isotropic and nematic uniaxial-to-biaxial phase transitions in a lyotropic liquid crystal. In the *N-I* transition, the nonlinear optical birefringence shows a discontinuity in T_c, as observed in the linear birefringence. On the other hand, in the N_C-to-N_B transition, Δn_2 was shown to be proportional to $|T-T_{c1}|^{-\beta}$, with $\beta\sim0.5$. No discontinuity was observed on Δn_2 in the N_C-to-N_B transition. The symmetric invariants of the order parameter were shown to be linear functions of the temperature in the temperature range of $\Delta T/T_{c1}\sim7\times10^{-3}$ and 2×10^{-2}, corresponding to the N_C and N_B phases, respectively, in good agreement with the mean-field prediction.

ACKNOWLEDGMENTS

Fundação de Amparo à Pesquisa do Estado de São Paulo supported this work.

[1] L.J. Yu and A. Saupe, Phys. Rev. Lett. **45**, 1000 (1980).
[2] R. Bartolino *et al.*, Phys. Rev. A **26**, 1116 (1982).
[3] E.A. Oliveira, L. Liébert, and A.M. Figueiredo Neto, Liq. Cryst. **5**, 1669 (1989).
[4] P. Tolédano and A.M. Figueiredo Neto, Phys. Rev. Lett. **73**, 2216 (1994).
[5] Y. Galerne and J.P. Marcerou, Phys. Rev. Lett. **51**, 2109 (1983).
[6] A. Saupe, P. Boonbrahm, and L.J. Yu, J. Chim. Phys. Phys.-Chim. Biol. **80**, 7 (1983).
[7] G. Melnik, P. Photinos, and A. Saupe, Phys. Rev. A **39**, 1597 (1989).
[8] J.C. le Guillon and J. Zinn-Justin, Phys. Rev. Lett. **39**, 95 (1977).
[9] M.B. Lacerda Santos, Y. Galerne, and G. Durand, Phys. Rev. Lett. **53**, 787 (1984).
[10] M. Sheik-Bahae *et al.*, IEEE J. Quantum Electron. **26**, 760 (1990).
[11] S.L. Gómez *et al.*, Phys. Rev. E **59**, 3059 (1999).
[12] P. Palffy-Muhoray *et al.*, Mol. Cryst. Liq. Cryst. **207**, 291 (1991).
[13] L.C. Oliveira and S.C. Zilio, Appl. Phys. Lett. **65**, 2121 (1994).
[14] Y. Galerne, A.M. Figueiredo Neto, and L. Liébert, J. Chem. Phys. **87**, 1851 (1987).
[15] F.L.S. Cuppo *et al.*, J. Opt. Soc. Am. B **19**, 1342 (2002).
[16] J.R.D. Pereira *et al.*, Phys. Rev. E **64**, 062701 (2001), and references therein.